Magnetic properties of isolated Rh and Ru impurities in Pd and Pd-Fe: A theoretical study

M. R. Press, S. N. Mishra, S. H. Devare, and H. G. Devare
Tata Institute of Fundamental Research, Homi Bhabha Road, Bombay 400 005, India
(Received 12 October 1992)

We perform self-consistent electronic-structure calculations to investigate the possible existence and formation mechanism of local magnetism in isolated late-4*d* transition-metal impurities in Pd and dilute Pd-Fe alloys, using the local-spin-density approximation and the cluster model for simulating the bulk. We find that Ru in Pd exhibits a giant moment of $4\mu_B$, but reduced in magnitude compared to its 3*d* counterpart Fe in Pd. Tc and Rh in Pd turn out to be nonmagnetic, the latter in disagreement with time-differential perturbed-angular-correlation (TDPAC) experiments, which suggest a reduced giant moment per Rh atom also. The self-consistent small *d*-band splittings in the primary ferromagnetic impurity-host *d*-*d* hybridization allow for an electronic exchange conversion mechanism, varying in extent across the 4*d* series, with consequent reduction in the impurity-site local moment and in the host-*d* spin polarization. The effective suppression of the spin fluctuations from the impurity-host *d*-*sp* interaction is thereby also undermined, resulting in high spin-fluctuation temperatures T_K. In very dilute Pd-Fe alloys, a local moment of $\sim 1\mu_B$ is seen to stabilize at the Rh or Ru site when in the polarization cloud surrounding an Fe atom. The enhancement in the exchange splitting and in the host-*d* polarization, producing an extensive polarization cloud with a giant moment, suggests a decrease in T_K. At higher Fe concentrations, decoration of the probe with Fe atoms results in polarization clouds with ultralarge stabilized local moments, also observed via TDPAC, which increase in jumps of at least the $\sim 3.4\mu_B$ *d* moment on each Fe atom.

I. INTRODUCTION

There is a profuse and steadily growing body of literature[1] on the magnetic properties of 3*d* and 4*d* transition metals when doped or alloyed with other transition metals. On the experimental front, extensive studies have been made using widely differing techniques that have made possible impurity concentrations and compositions of all orders. Of these, the time-differential perturbed γ-ray angular distribution and correlation (TDPAD and TDPAC) methods,[2] when coupled with ion implantation, have proved to be particularly precise and powerful techniques for probing local magnetic properties in extremely dilute limits, even in hosts where alloying through more conventional methods is difficult or not possible. They have been used to study the possible existence, stability, and spin dynamics of local magnetic moments on transition metals in *sp*-, noble, and other transition-metal hosts.[3,4]

Theoretical investigations since the early 1960s into the problem of localized magnetic moments in metallic hosts have taken several different approaches, but have left many important questions unanswered. In the virtual-bound-state (vbs) model[5] introduced by Friedel and developed by Anderson, the transition-metal impurity *d* level is broadened by interaction with the host conduction band giving a resonance near the Fermi energy; competition between the intra-atomic correlation energy and the *d*-*sp* hybridization then determines the possible existence and strength of the local magnetism. In the Kondo theory[6] of the resistivity of dilute alloys, magnetic moments are screened by correlations with the conduction electrons below a characteristic temperature and do not manifest themselves. The theory of spin fluctuations,[7] which was developed to explain the T^2 behavior of the resistivity in the $T \rightarrow 0$ limit in some alloys, unaccounted for in the Kondo theory, introduces a lifetime τ for the impurity spin, the magnitude of which determines the stability of the moment. These ideas have currently been brought together in the stipulation of a characteristic temperature T_K which delineates the regimes of manifestation of stable magnetic moments (above T_K) and of reduced or nonmagnetic behavior (below T_K). Still, in the absence of a microscopic description of the moment, an experiment yielding a null magnetism result leaves open the question of whether a magnetic moment is screened or fluctuating rapidly, or simply does not exist at all chemically.[8] In recent years, the efficacy of *ab initio* approaches based on the local-spin-density (LSD) formalism,[9] such as the Green's function KKR method[10] and the embedded-cluster method,[11] which investigate the electronic structure and magnetic properties of impurities in metals, has been well established. At present, these self-consistent approaches represent our best hope of providing a microscopic mechanism of moment formation, besides supplying reliable values of parameters to be used in different model systems.

Pure Pd exhibits a strongly exchange-enhanced susceptibility with a Stoner enhancement factor of ~ 4.5 (Ref. 12), which makes it an incipient ferromagnet. Magnetic 3*d* impurities in Pd (Ref. 13) exhibit stable greater than bulk magnetic moments at the impurity site and produce

0163-1829/93/47(22)/14988(10)/$06.00

large host polarizations extending spatially over $\gtrsim 100$ Pd atoms; these are the well-studied so-called giant moment systems, driven by strong impurity-host d-d coupling. Gross, Riegel, and Zeller[14] have studied magnetic-moment formation and spin dynamics of isolated $4d$ ions in Pd, both experimentally using the TDPAD technique and theoretically via the Green's function method based on the LSD formalism. They observe nonmagnetic behavior for Mo and Tc ions in Pd, whereas Ru and Rh are found to be strongly magnetic, even suggestive of giant $4d$ moment formation in Pd. The local susceptibility $\beta(T)-1$, extracted from the spin rotation patterns and the Larmor frequency, exhibits a typical Curie-Weiss-type response $\beta(T)-1\simeq C/(T+T_K)$. It is found that $\beta(T)<1$, signifying a predominantly effective spin magnetic moment; and the derived spin-fluctuation temperature T_K has a rather high value between 200 and 300 K, suggesting the quasistable nature of the moment. The accompanying theoretical calculations on these systems severely underestimate the magnitude of the magnetic effects; e.g., Rh turns out to be nonmagnetic and the total moment for the Ru site, even with the application of a magnetic field, is $\sim 1\mu_B$, much less than the experimental estimate of $\gtrsim 5\mu_B$. Clearly somewhat different mechanisms are operative between the $3d$ and $4d$ impurity cases, and the above discrepancy between theory and experiment for the $4d$ ions in Pd is worth investigating. More recently, the local magnetic behavior of isolated Rh impurities in paramagnetic Pd-Fe alloys has been reported.[15] It is seen that the spin-fluctuation temperature T_K in the parametrization of $\beta(T)$ drops sharply with the addition of even very small amounts ($\sim 0.2\%$) of Fe into Pd and further reduces to zero with increasing Fe concentration ($\gtrsim 1\%$). This implies that the erstwhile quasistable Rh moment in Pd becomes highly stable ($T_K \rightarrow 0$) in the Pd-Fe alloy and a giant moment system ensues.

In the present work, we perform self-consistent electronic-structure calculations for molecular clusters representing isolated late-$4d$ transition-metal (Pd, Rh, Ru, and Tc) impurities in Pd, and for single Rh and Ru probes in dilute Pd-Fe alloys. We consider a typical 19 atom cluster $M_1M_{12}M_6$ ($M\equiv$ metal atom) comprising two full coordination shells of atoms around a central atom in fcc lattice geometry. The Pd-Fe alloys of varying low Fe concentration are simulated by substitution of one or more Pd atoms by Fe atoms. Since the experimental spectra show evidence that the implanted ions come to occupy substitutional sites in the host Pd and Pd-Fe lattices, similar site substitution of Pd by Rh or Ru, in the presence of Fe atom decoration within the cluster if necessary, is an adequate model for studying the Rh-(Ru-) Fe-Pd interaction. From these spin-polarized calculations, the existence and magnitude (when present) of local magnetic moments can be determined, as well as the role of local electronic bonding in their formation and stability.

In Sec. II, we briefly outline our method of investigation, follow up with a presentation and discussion of our results in Sec. III, and summarize our main findings in the conclusion.

II. THEORETICAL-COMPUTATIONAL PROCEDURE

The self-consistent local-density functional discrete variational (DV) LCAO method[16] for bulk studies employed here has been described in good detail elsewhere, so only those aspects relevant to the present calculation will be presented in this paper. Essentially, a suitable chunk of the bulk is chosen for explicit self-consistent description as a cluster of atoms, while the rest of the crystal manifests its presence by providing a crystal field in which the cluster is embedded. The nonrelativistic one-electron Hamiltonian for a cluster of atoms is given in Hartree atomic units by

$$H(\mathbf{r})=(-1/2)\nabla^2+V_C(\mathbf{r})+V_{\mathrm{XC}}^{\sigma}(\mathbf{r}) . \tag{1}$$

Here $V_C(\mathbf{r})$ is the electron-electron cum electron-nucleus Coulomb potential. The local spin-dependent potential $V_{\mathrm{XC}}^{\sigma}(\mathbf{r})$ for exchange-correlation is chosen to be of the spin-polarized form derived by von Barth and Hedin.[17] Molecular-orbital (MO) eigenfunctions $\phi_{i\sigma}(\mathbf{r})$, which solve the above Hamiltonian via a self-consistent iterative procedure, are expanded in terms of symmetrized linear combinations of atomic orbitals, $\psi_j(\mathbf{r})$,

$$\phi_{i\sigma}(\mathbf{r})=\sum_j C_{ij}^{\sigma}\psi_j(\mathbf{r}) . \tag{2}$$

The variational basis consists of numerical free-atom orbitals obtained from density-functional calculations and centered on each cluster atom. For the $4d$ elements, only the $4d$, $5s$, and $5p$ orbitals are treated variationally, and similarly the $3d$, $4s$, and $4p$ orbitals for the $3d$ elements. The deeper lying orbitals, $1s\ldots 4p$ and $1s\ldots 3p$ for $4d$ and $3d$ elements respectively, are treated as "frozen core" or nonvariational. Previous work has shown that this near-minimal basis has sufficient variational freedom to describe compact structures such as found in the bulk, and that the frozen-core approximation does not affect the potential field generated, nor the charge polarization and magnetic properties derived from states near the Fermi energy. This yields the usual variational secular equation

$$(\underline{H}_{\sigma}-\epsilon_{\sigma}\underline{S})\underline{C}^{\sigma}=\underline{0} . \tag{3}$$

The spin-dependent Hamiltonian matrix $\underline{H}_{\sigma}$ and the overlap matrix $\underline{S}$ are evaluated as weighted sums over a set of discrete three-dimensional pseudorandom sampling points $\mathbf{r}_{\mathbf{k}}$ to yield the one-electron eigenvalues $\epsilon_{i\sigma}$ and the spin densities

$$\rho_{\sigma}(\mathbf{r})=\sum_i f_{i\sigma}|\phi_{i\sigma}(\mathbf{r})|^2 . \tag{4}$$

The occupation numbers $f_{i\sigma}$ are chosen according to a Fermi-Dirac distribution with a slight thermal broadening corresponding to 100 K to aid convergence of cluster orbital energy levels near the Fermi energy. Contributions to the spin density come from unpaired orbital spins as well as from the differing spatial distributions of cluster spin orbitals in responding to the spin-dependent potentials. One can now obtain the exact cluster charge density $\rho(\mathbf{r})=\rho_{\uparrow}(\mathbf{r})+\rho_{\downarrow}(\mathbf{r})$ and the spin magnetization

density $\delta\rho(\mathbf{r})=\rho_\uparrow(\mathbf{r})-\rho_\downarrow(\mathbf{r})$. To construct the potential, the cluster charge density is remodeled by projecting onto multicenter atomic radial functions,

$$\rho_\sigma^{\text{model}}(\mathbf{r})\simeq\sum_{v,nl}A_{nl}^{v\sigma}|R_{nl}(\mathbf{r}_v)|^2\ , \tag{5}$$

where the occupation numbers $A_{nl}^{v\sigma}$ for the atomic orbital R_{nl} with quantum numbers n and l on atom v are obtained via a Mulliken population analysis of the cluster charge density. Magnetic moments at particular sites are then quoted as the difference between spin-up and spin-down Mulliken populations. The embedding scheme consists of placing free-atom potentials at all lattice sites outside the cluster within a radius of twice the lattice constant a. Its presence or absence has a negligible effect on the charge distribution within the cluster and on the d-electron density of states of the surface atoms. Finally, to treat the cluster MO states as analogs of solid-state bands and for comparison with spectroscopic data, we broaden the cluster level at $\epsilon_{i\sigma}$ by a Lorentzian of suitable half-width $\gamma=0.4$ eV to define a local, or site-projected, spin density of states (DOS) $D_\sigma^v(\epsilon)$,

$$D_\sigma^v(\epsilon)=\sum_{i,nl}A_{nl}^{v\sigma}\frac{\gamma/\pi}{(\epsilon-\epsilon_{i\sigma})^2+\gamma^2}\ . \tag{6}$$

The self-consistent molecular orbitals are spatially extended throughout the cluster and can be expected to describe local regions of polarization within the cluster. As long as the cluster size is comparable to or larger than the sampling size of the particular experiment, our method could in principle determine whether the properties seen by the experiment are of a localized nature or are delocalized, the latter necessarily requiring description by states extending throughout the solid. Thus cluster size is an important constraint in relation to both the experimental technique and the volume over which the cluster is simulative of the properties of the bulk. Considering the size of the 19-atom cluster we use, we find that the charge and spin densities associated with the central atom M_1 is representative of the bulk. However, the M_{12} shell to a certain extent, and the M_6 shell to a greater extent, are subject to spurious "surface" effects. That is, since their coordination shells within the cluster are incomplete, having only 7 and 4 atoms respectively rather than 12, hybridization and orbital overlap leading to bulklike spin quenching are reduced. The spin polarizations calculated for these atoms are therefore higher than their values in the bulk. We shall therefore concentrate mainly on the central impurity site, hereafter also referred to as the probe site. Thus, the outer shells are adequate in providing an explicitly treated self-consistent environment for the central region of the cluster, but our approach is limited in its treatment of perturbations on the near-neighbor Pd or Fe atoms around the central probe atom. This complication due to cluster size must be factored into any interpretation of our results.

III. RESULTS AND DISCUSSIONS

A. In the host Pd

In Table I we present the spin magnetic moments calculated at the $4d$ impurity site, at the nearest-neighbor (nn) Pd site, and the total moment for the cluster of 19 atoms. In the panel series [Figs. 1(a)-1(d)], we show the local density of states (DOS) for both spins for the host Pd as obtained at the Pd_1 site, as well for the Rh, Ru, and Tc sites in Pd. Pd crystallizes in the fcc structure with $a=3.89$ Å. The atomic radius of the other $4d$ transition-metal elements considered here is within ±0.03 Å of Pd's ($r_a=1.37$ Å), so no significant local lattice relaxation around the impurity is expected upon implantation. The host Pd is seen to be cleanly paramagnetic; the DOS for both spins are nearly identical and their integrated difference gives $\mu=0\mu_B$. Bonding and antibonding orbitals of d character are centered around -4.5 and -0.5 eV relative to the Fermi energy E_F giving a net d-band width of ~5 eV. These features are consistent with the DOS obtained by Moruzzi *et al.*[12] via a local-density band-structure calculation, though our upper d band has somewhat less weight. The nominal ground-state configuration for free Pd atoms is $4d^{10}$, but our self-consistent Mulliken orbital occupations for the bulk representative Pd_1 site are $4d^{9.30}5s^{0.22}5p^{0.48}$. The 0.7 hole in the d band accounts for the spillover of d character above E_F and is in agreement with estimates from

TABLE I. Summary of calculated orbital and total magnetic moments for isolated $4d$ metal atoms in Pd. μ_1 and μ_{12} are the local moments at the d metal site and the nn Pd site; their values from a previous calculation (Ref. 14) are given in brackets. Contributions to μ_1 from $4d$, $5s$, and $5p$ orbitals are also given. μ_{tot} is the total moment over all 19 atoms of the cluster; experimental values from Refs. 14 and 15 for the net polarization cloud moment are shown in brackets alongside.

System	Cluster employed	$\mu_1^d+\mu_1^s+\mu_1^p=\mu_1(\mu_B)$	μ_{12} (μ_B)	μ_{tot} (μ_B)
Pd in Pd	$Pd_1Pd_{12}Pd_6$	$0.00+0.00+0.00=0.00$	0.00	0
Rh in Pd	$Rh_1Pd_{12}Pd_6$	$-0.05-0.003-0.007=-0.06(0)$	0.045(0)	1(4.8)
Ru in Pd	$Ru_1Pd_{12}Pd_6$	$0.79+0.015+0.045=0.85(0.30)$	0.20(0.04)	4($\gtrsim5$)
Tc in Pd	$Tc_1Pd_{12}Pd_6$	$-0.03-0.003-0.007=-0.04(0)$	0.06(0)	1(0)

band-structure calculations that there are 0.4–0.6 holes in the d band of Pd. The Knight shift and paramagnetic susceptibility data on Pd (Ref. 18) can be described as a Curie-Weiss response with $C=-20$ K and $T_K=400$ K and are consistent with a d-band splitting corresponding to a 0.4 hole.

Our calculation for Rh in Pd, carried out effectively at 0 K, gives a null local moment $|\mu_1^d|<0.05\mu_B$ at the Rh site with an exchange splitting, or majority-minority band splitting ΔE_d in the Anderson model, of less than 0.02 eV. The negative value of μ_1^d is an artifact of the particular cluster size. For a 13-atom cluster Rh_1Pd_{12} we obtain $\mu_1^d=-0.22\mu_B$. From this trend, for a sufficiently large cluster we expect the local Rh moment to converge to a vanishingly small, or at most a small positive, value. The polarization of the nn shell of Pd atoms is also small, $\mu_{12}\approx\mu_{12}^d=0.045\mu_B$, but still on the higher side due to surface effects. The exact integral number for the calculated total spin moment $\mu_{\rm tot}$ for all cluster atoms is simply a consequence of using Fermi-Dirac statistics with occupation indices 1 or 0 for each molecular orbital, and of Rh having an odd number of electrons. Thus while the inner region of the cluster is representative of the bulk, the outermost M_6 surface shell adjusts to give an integral moment.

In a pioneering work using the TDPAC method to measure the Knight shift of ^{100}Rh in very dilute Pd-Rh alloys, Rao, Matthias, and Shirley[19] obtained a core-d hyperfine field $H_{hf}^d\sim-70$ T/spin at high temperatures $T\gtrsim400$ K and $H_{hf}^d\to0$ T/spin for $T\to0$ K. From the difference in the temperature dependence of the impurity Knight shift of Rh in Pd and the Knight shift in pure Pd, they drew the subtle deduction that in the low-temperature regime the polarization of the lattice due to the impurity is long ranged, while at higher temperatures a localized moment forms on the Rh atom. This temperature dependence of the local susceptibility can again be characterized by a Curie-Weiss law with $C=-30$ K and $T_K=210$ K, from which a net moment of $\sim4.8\mu_B$ for the Rh-Pd system has been derived[15] under reasonable assumptions. Narath and Weaver[20] contended from low-temperature NMR measurements of the ^{103}Rh Knight shift and spin-lattice relaxation rate that the enhancement in the Rh susceptibility can be attributed to the uniform exchange enhancement of the host due to the particular form of the DOS near E_F, rather than to the formation of a magnetic moment on Rh.

For Tc in Pd, too, the local impurity spin moment is nearly zero, $|\mu_1^d|<0.05\mu_B$, with an exchange splitting $\Delta E_d\lesssim0.02$ eV. This is consistent with its nonmagnetic behavior $\beta=1$ observed by Gross *et al.*[14]

Only Ru in Pd shows a substantial local spin moment $\mu_1^d=0.79\mu_B$ with $\Delta E_d=0.2$ eV, driving a correspondingly larger nn Pd polarization $\mu_{12}^d=0.21\mu_B$. Note also the small ferromagnetic polarization of the 5sp electrons on Ru and the slight but significant contribution from the

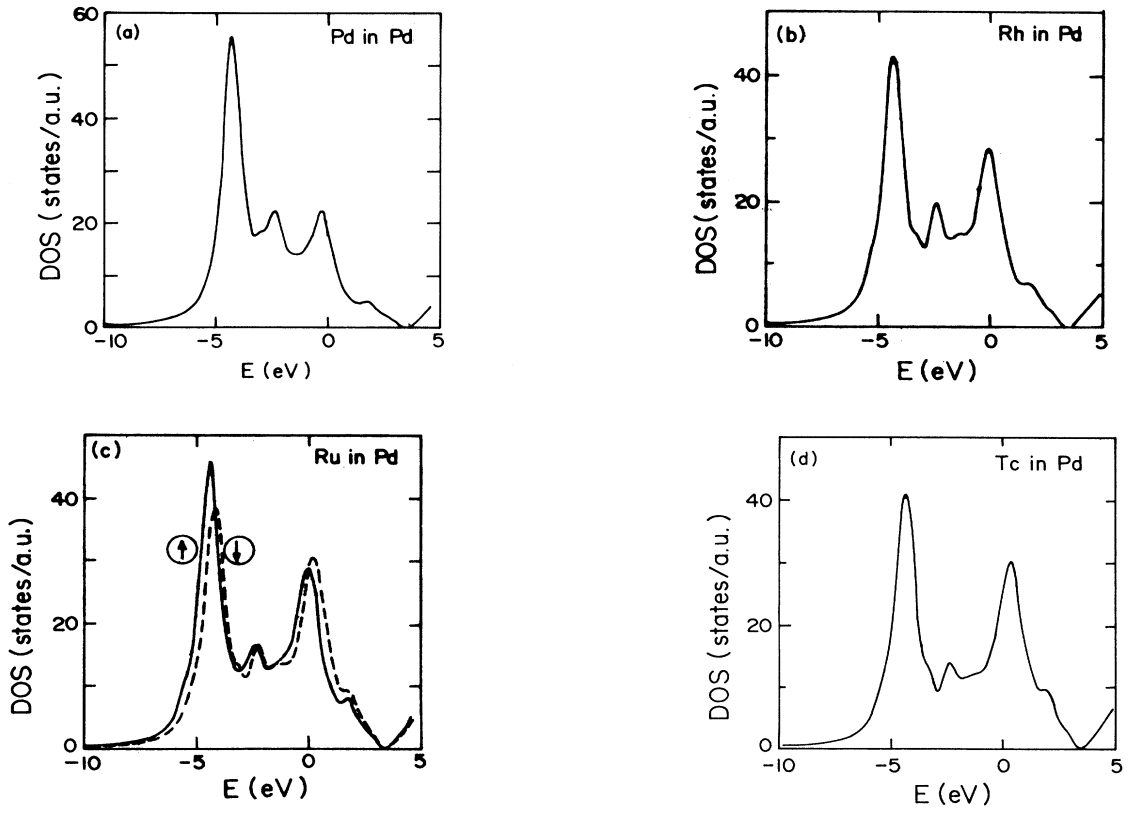

FIG. 1. Local density of states (DOS) for different 4d probes in Pd. (a) Pd, (b) Rh, (c) Ru, and (d) Tc.

opposite polarization of $5sp$ electrons on the Pd($\mu_{12}^s+\mu_{12}^p=-0.005\mu_B-0.005\mu_B$). The net moment per Ru atom, $\mu_{tot}=4\mu_B$, is slightly under the estimate of $\gtrsim 5\mu_B$ from TDPAD experiments.[14] In Fig. 2 we plot the difference in spin DOS $[D_\uparrow(\epsilon)-D_\downarrow(\epsilon)]$ at the Ru site and for Ru+Pd_{12}. There is a ponderance of minority antibonding hybrids up to ~2 eV above E_F. One can now clearly see in both figures the formation of a virtual bound state in the signature doublet structure straddling the Fermi energy. The host polarization shows typically as the strong extra oscillations in Fig. 2(b). These features, in the DOS as well as the signs and values for the local moments, are symptomatic of giant moment formation as in the case of magnetic $3d$ elements in Pd and we shall see later that Ru-Pd is indeed a "reduced" giant moment system. The impurity-host d-d coupling results in the host-d polarization adding up to an enhanced moment; in the conventional Kondo picture, it suppresses the spin fluctuations associated with the antiferromagnetic d-sp interaction which serves both to screen and effectively reduce the Ru moment as well as to undermine its stability.

The main features of the local DOS across the $4d$ transition series are quite similar, except for a gradual shift across E_F towards higher energy in the position of the antibonding hybrids in going from Pd-Pd to Tc-Pd.

Before attempting to understand these results, let us first appreciate the similarities and differences in local moment formation between the late-$4d$ and late-$3d$ elements in the host Pd. To this effect, we have also carried out calculations identical to the above for isolated magnetic $3d$ impurities, Ni, Co, Fe, and Mn, in Pd. The results are presented in a comparable manner in Table II. We shall discuss only the case of Fe in detail since it is relevant to our following section on dilute Pd-Fe alloys also. The DOS at the Fe site in Fig. 3 shows multiple peak structures for both spins in a valence band extending 6 eV below the Fermi energy. In this region, the minority spins have consistently smaller magnitudes than the majority spins; just above E_F for 2 eV, however, there is considerable d character coming from minority antibonding hybrids. The exchange splittings are about 0.45 and 1.3 eV, respectively, for the majority and minority

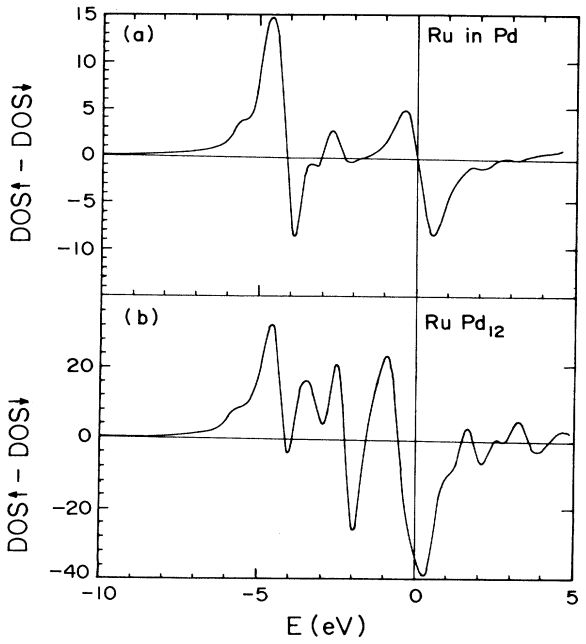

FIG. 2. Spin-difference density of states in units of states (a.u.) for the Ru-Pd system. (a) The Ru site and (b) Ru-Pd_{12}.

bands. The integrated differences in the spin DOS gives a net local moment of $3.59\mu_B$ on Fe. Across the magnetic $3d$ series, our results predict in each case a local $3d$ spin moment μ_1^d, which is intermediate between the lower bulk value and the free-atom value (e.g., $3.25\mu_B$ for Fe is between 2.2 and $4.0\mu_B$). Note also that the contribution $\mu_1^s+\mu_1^p$ from $4s+4p$ orbitals is non-negligible and scales with μ_1^d, ranging from 6–11 % of μ_1^d in going from Ni to Mn. The values for the local impurity moment μ_1 are in good agreement with those obtained by Oswald *et al.*[13]

The polarization μ_{12} on the nn Pd arises from its d-band splitting dictated by the placement of the minority band above E_F due to the presence of the Fe. Its magnitude, $0.19\mu_B$ for Fe in Pd, is again on the higher side possibly due to surface effects. In an earlier work Delley

TABLE II. Summary of calculated orbital and total magnetic moments for isolated $3d$ metal atoms in Pd. μ_1 and μ_{12} are the local momenta at the d metal site and the nn Pd site; their values from a previous calculation (Refs. 13, 14) are given in brackets. Contributions to μ_1 from $3d$, $4s$, and $4p$ orbitals and to μ_{12} from $4d$, $5s$, and $5p$ orbitals are also given. μ_{tot} is the total moment over all 19 atoms of the cluster; experimental values for the net polarization cloud moment, quoted in Ref. 13, are shown in brackets alongside.

System	Cluster employed	$\mu_1^d+\mu_1^s+\mu_1^p$ $=\mu_1(\mu_B)$	$\mu_{12}^d+\mu_{12}^s+\mu_{12}^p$ $=\mu_{12}(\mu_B)$	$\mu_{tot}(\mu_B)$
Ni in Pd	$Ni_1Pd_{12}Pd_6$	0.85+0.02+0.03 =0.90(0.92)	0.235−0.005−0.01 =0.22(0.063)	6(4.6±1.8)
Co in Pd	$Co_1Pd_{12}Pd_6$	2.13+0.06+0.12 =2.31(2.28)	0.35−0.015−0.015 =0.32(0.114)	7(9−10)
Fe in Pd	$Fe_1Pd_{12}Pd_6$	3.25+0.11+0.23 =3.59(3.47)	0.24−0.03−0.02 =0.19(0.102)	8(10−13)
Mn in Pd	$Mn_1Pd_{12}Pd_6$	4.05+0.14+0.31 =4.50(4.13)	0.14−0.035−0.02 =0.085(0.048)	7(6.5−8)

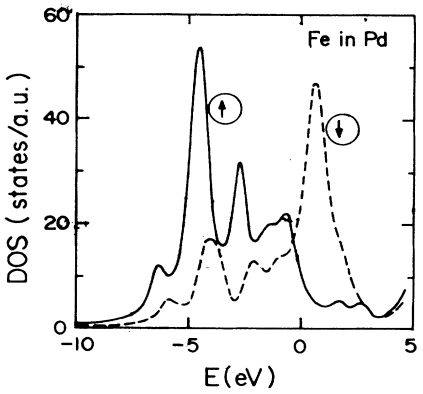

FIG. 3. Local density of states (DOS) for Fe atom in Pd.

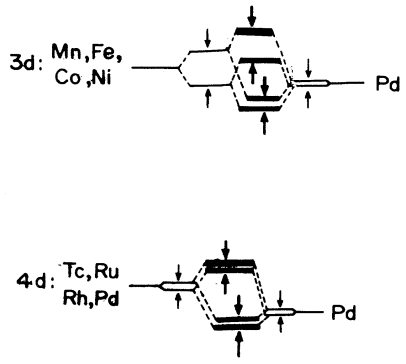

FIG. 4. A simple model for d-d hybridization in the basic probe-Pd interaction.

et al.[21] obtained similar results for the Fe-Pd system using the same DV-LCAO procedure and nearly identical parameters as employed here. It is shown there that not until one considers a 55-atom cluster $Fe_1Pd_{12}Pd_6Pd_{24}Pd_{12}$ does the nn Pd polarization reduce from 0.19 to $0.125\mu_B$. The reason quite simply is that a 55-atom cluster is the smallest cluster for which the nn Pd atoms have a full coordinating shell of atoms within the cluster, and hence fairly complete hybridization of orbitals and spin quenching. A similar result can also be stimulated with a 28-atom cluster made up of two overlapping 19-atom clusters centered around adjacent Fe and Pd atoms. About the polarization of Pd neighbors further out, our calculations can realistically say nothing; the size of our cluster restricts us to sampling only one shell of the polarization cloud at best. (A similar scenario could be valid experimentally too: the giant moment for trace Fe in Pd has been estimated to be $8-13\mu_B$ from different experimental methods, the range reflecting the volume of the polarization cloud that the probe technique accesses.) Delley *et al.*[21] have shown that in going to larger clusters (19, 43, and 55 atoms), it is always the outermost shell of atoms which adjusts in polarization so that (a) successively larger inner regions of the cluster have their magnetic moments reliably reproduced, and (b) the net moment on the cluster μ_{tot} is maintained constant, for instance $8\mu_B$ for Fe-Pd. Note that the experimental trend in magnitude of the giant moment across the $3d$ series is reproduced by μ_{tot}, both given in the last column of Table II.

The magnitude of the local moments at the $3d$ site and the induced polarizations on the nearby Pd sites can be understood in a straightforward manner in terms of the LCAO-MO scheme and the energy levels of the two atomic species involved. Starting with the spin-dependent $3d$ atomic levels for the magnetic impurity and the $4d$ atomic levels for a host Pd atom, we show schematically in Fig. 4 how a discrete set of molecular orbitals form due to impurity-host interactions between spin-up (or majority) and spin-down (or minority) states. As a consequence of coupling and hybridization, the d orbitals split into bonding and antibonding states, each capable of accommodating up to 10 electrons, and which are to be filled with electrons as per the Aufbau principle and Fermi-Dirac statistics. Since there are between 15 and 19 electrons in going from the Mn-Pd to the Ni-Pd interactions, all the bonding hybrid states in the valence region and the antibonding majority hybrids are filled. As the minority antibonding hybrids fill up, one would expect the overall moment to decrease from approximately $5\mu_B$ for Mn-Pd to $1\mu_B$ for the Ni-Pd interaction. The spin-up orbitals have substantially larger amplitude or projection at the impurity site, so that Fe, for instance, ends up with a local moment μ_1^d of $3.25\mu_B$ and the nn Pd with a polarization μ_{12}^d of $\lesssim 0.24\mu_B$. This, along with the much reduced polarization on the further neighbor Pd atoms, yields an extensive polarization moment cloud. Thus strong ferromagnetic d-d interaction is found adequate to account for giant moment formation for $3d$ metal atoms in Pd; it overwhelms the destabilizing impurity-host d-sp exchanges and accounts for the very low T_K values ($\sim 10^{-3}$ K for Fe in Pd).

The situation in the $4d$ series is more involved. In the case of the Rh-Pd and Ru-Pd interactions, one would expect, in analogy with the above analysis, net moments of ~ 2 and $\sim 3\mu_B$ respectively, as 18 and 17 d electrons are to be accommodated in the bonding and antibonding hybrids. However, the greater spatial extent of the impurity $4d$ orbitals causes stronger overlap and hybridization with the valence band of Pd. Also, to begin with, the nonmagnetic nature of the impurity atoms would lead to smaller exchange splittings. The minority antibonding states are thus brought lower in energy to couple more strongly with the valence band of Pd. In filling up the orbitals with the total charge in the M-PD system, some charge has to be accommodated in empty states near E_F which are mainly of minority-spin character. So a mechanism[22] is set up whereby spin-up charge is transferred to minority-spin levels without requiring d electron or charge transfer or raising or lowering of the Fermi energy. In the LCAO-MO picture, this amounts to an overall exchange conversion of one electron and its accommodation as a spin-down electron in the minority band, thereby reducing the net moment by $2\mu_B$ to $\sim 0\mu_B$ for the Rh-Pd and $\sim 1\mu_B$ for the Ru-Pd interactions. Though

Ru is nearly isoelectronic to Fe in the Pd matrix ($4d^{6.98}$ to $3d^{6.76}$), the spin-flip mechanism leads to a reduced local moment at the Ru site and also a reduced giant moment overall for the Ru-Pd system. The reduced exchange splitting and host-d polarization are that much less competitive against the destabilizing d-sp interaction and suggest why the spin-fluctuation temperature T_K is a high 280 K. For Tc in Pd, there is provision for the exchange conversion of two electrons, since the extension of the $4d$ orbitals is maximum towards the center of the $4d$ series where it is most open. For Rh and Tc in Pd, it is not energetically favorable for the system to polarize and they are therefore nonmagnetic by our calculations. Considering the discrepancy with experiment for the Rh-Pd system, it is possible that a magnetic solution for Rh-Pd is close in energy to our present null moment result. Such a result would feature exchange conversion of a fraction of an electron; this partial arrest is made plausible by noting that the spread and hybridization of the $4d$ orbitals are reduced as the $4d$ series closes. We have thus identified the extra complication in $4d$ moment formation and stability in Pd, beyond the mechanism operative for $3d$ moment formation in Pd.

B. In dilute Pd-Fe alloys

The same 19-atom cluster as above, in reduced symmetry, has been used to study formation and stability of local moments on single Rh and Ru probes in dilute Pd-Fe alloys. By substituting Pd atoms strategically with Fe atoms at suitable sites, the clusters can be made representative of Pd-Fe alloys of varying low Fe concentrations. The probe Rh or Ru atom is always at the central M_1 site. Several intriguing questions remain. How sensitive is the local moment to proximity of an Fe atom? What is the effect of Fe atom decoration on the local moment and on the polarization of the Pd? To what degree does the polarization on the Pd atoms grow? What is the mechanism for enhanced stability of the moments? In what follows we attempt to address just these questions. In Table III, we show the site-specific orbital and total magnetic moments, rounded off to the nearest $0.005\mu_B$, for Rh and Ru impurities in a Pd matrix in the presence of one or more Fe atoms within the cluster. We study three cases pertaining to the experimental situation.

(1) A Rh or Ru probe atom at second nn distance $d=a=3.89$ Å from a single Fe atom, typical of very low Fe concentration. A substantial local d moment of magnitude $0.95\mu_B$ is seen to stabilize at the Rh site, while the Ru d moment increases marginally from its $0.79\mu_B$ value in pure Pd to $0.95\mu_B$. This is accompanied by minimal charge transfer and change in the occupation of the $4d$ orbitals. A moment of $1\mu_B$ on Rh has been observed[23] via neutron diffraction in crystalline binary Fe_xRh_{1-x} for $x\sim 2/3$; a LSD band-structure calculation[24] of Fe-Rh in the CsCl structure also yielded a ferromagnetic solution with local moments of $1\mu_B$ on Rh and $3\mu_B$ on Fe. We have also plotted the spin DOS and the spin difference DOS for Rh and Ru in this situation in Figs. 5 and 6, respectively. Both sets of DOS are seen to be remarkably similar. Note the enhanced state density for both spins for up to 5 eV and more above E_F as also the ponderance of minority-spin states just above E_F, signalling the appearance of a vbs. The mechanism is indeed quite similar to that which gave giant moments in Fe-Pd, and is applicable also to the two situations following. That is, the presence of Fe places a band of antibonding minority hybrids above E_F for up to 2.5 eV. Multiple coupling and overlap between the d states of Rh or Ru, Pd, and Fe leads to some electrons being accommodated in the vbs above E_F. Some of these electrons have amplitude on the probe atom, so that an exchange splitting results and a local moment develops at the Rh or Ru site. This scenario is expected to be valid even for Fe in further neighbor positions of the probe, as long as the probe lies within the polarization cloud of an Fe atom. This also serves to increase the polarization on the probe's nn Pd atoms beyond that found for a single Fe or a single probe atom in Pd, as some spin-down electrons having amplitude on

TABLE III. Summary of calculated orbital and total magnetic moments in Bohr magnetons (μ_B) for isolated Rh and Ru impurities in Pd in the presence of one or more substitutional Fe atoms. μ_1, $\langle\mu_{12}(\mathrm{Pd})\rangle$ and $\mu(\mathrm{Fe})$ are the local moments at the Rh or Ru site, the average polarization on the nn Pd site, and the Fe atom local moment, respectively. Contributions to the local moments from d and $s+p$ orbitals are also shown. μ_{tot} is the contribution to the overall moment of the polarization cloud from the impurity atom, its nn Pd atoms, and the Fe atoms decorating the impurity.

Cluster description	$d(M_1-\mathrm{Fe})$ symmetry	$\mu_1^d+\mu_1^s+\mu_1^p=\mu_1$	$\langle\mu_{12}^d\rangle+\langle\mu_{12}^{sp}\rangle=\langle\mu_{12}(\mathrm{Pd})\rangle$	$\mu^d+\mu^{sp}=\mu(\mathrm{Fe})$	$\mu_{\mathrm{tot}}^d+\mu_{\mathrm{tot}}^{sp}=\mu_{\mathrm{tot}}$
$Rh_1(Pd_4Pd_4Pd_4)$	3.89 Å	0.95+0.02+0.035	0.30−0.03	3.37+0.23	7.92−0.075
$(Pd_4Pd_1Fe_1)$	C_{4v}	=1.005	=0.27	=3.60	=7.845
$Rh_1(Pd_8Pd_4)$	3.89 Å	1.06+0.025+0.03	0.32−0.09	3.41+0.30	18.54+0.175
(Pd_2Fe_4)	C_{4v}	=1.115	=0.23	=3.71	=18.715
$Rh_1(Pd_8Pd_2Fe_2)$	2.75 Å	0.73−0.001+0.01	0.215−0.03	3.41+0.30	9.70+0.31
(Pd_4Pd_2)	C_{2v}	=0.74	=0.185	=3.71	=10.01
$Ru_1(Pd_4Pd_4Pd_4)$	3.89 Å	0.95+0.025+0.045	0.24−0.03	3.36+0.235	7.19−0.055
$(Pd_4Pd_1Fe_1)$	C_{4v}	=1.02	=0.21	=3.595	=7.135
$Ru_1(Pd_8Pd_4)$	3.89 Å	0.85+0.025+0.025	0.25−0.09	3.42+0.25	17.53−0.03
(Pd_2Fe_4)	C_{4v}	=0.90	=0.16	=3.67	=17.50
$Ru_1(Pd_8Pd_2Fe_2)$	2.75 Å	0.55−0.003+0.008	0.16−0.035	3.395+0.30	8.94+0.255
(Pd_4Pd_2)	C_{2v}	=0.555	=0.125	=3.695	=9.195

the Pd atoms are also accommodated in the vbs. The Pd atoms in the nn shell around the probe are no longer equivalent and must be treated independently. We therefore choose to summarize their different polarizations in terms of an average value $\langle \mu_{12}(\mathrm{Pd}) \rangle$. Its value is consistently larger for the Rh-Pd than for the Ru-Pd system by $\sim 0.06 \mu_B$ for all the cases considered here, consistent with a slightly higher average exchange parameter ΔE_d for the former. We can now point to the enhanced host-d polarization arising from the greater d-band splitting as responsible for the suppression in the spin-fluctuation temperature T_K. The redistribution within the local Fe atom moment $\mu(\mathrm{Fe})$, larger d and smaller sp moments, can be attributed to the extreme outer position of the Fe in the cluster, and not to any real perturbation of Fe by the presence of the probe. With two polarizing centers, the polarization cloud is now wider in extent than for just a single Fe or a single probe in Pd. The quantity μ_{tot}, therefore, is our partial estimate for the total moment per impurity atom, and is a sum over the local moments on the impurity, the nn Pd, and the number of Fe atoms associated with the impurity.

(2) A Rh or Ru probe surrounded by four Fe atoms at $d = a = 3.89$ Å. This configuration addresses the effects of decoration of the impurity by more than one Fe atom and becomes statistically significant at higher Fe concentrations. The effect of decoration on the local impurity moment of case (1) is slight: μ_1^d at the Rh site increases by $0.11 \mu_B$, while for Ru it decreases by $0.10 \mu_B$. The average d polarization $\langle \mu_{12}^d(\mathrm{Pd}) \rangle$ of the nn Pd around the probe atoms also is seen to increase only slightly by $\sim 0.02 \mu_B$ upon decoration. This suggests that the polarization of the Pd atoms tends to saturate upon decoration rather than continue to increase in some proportion, the limiting criterion being the magnitude of the d-band hole. Accepting that the same mechanism as in case (1) is operative here, these perturbations are consequences of the subtle relocation of the antibonding orbitals in self-consistent adjustment to the presence of the extra Fe atoms. The huge increase to the ultralarge total moment μ_{tot} is due mostly to the $\sim 3.4 \mu_B$ d moment on each Fe atom. Still, the increase in the host-d polarization and consequent extension of the polarization cloud suggests further reduction in T_K over case (1).

The magnitude of the local moment appears to depend on the relative strengths of the Rh-Fe and Rh-Pd interactions. It will therefore vary with the proximity of the probe to the Fe atoms and their decoration number. The characters of the two interactions in the bulk are significantly different. It is straightforward to see in filling up the hybrid orbitals that the former can sustain local moments of $\sim 1 \mu_B$ at the Rh site and $\sim 3 \mu_B$ at the Fe site, with a large enough exchange splitting to inhibit the kind of spin-flip mechanism prevalent in the Rh-Pd

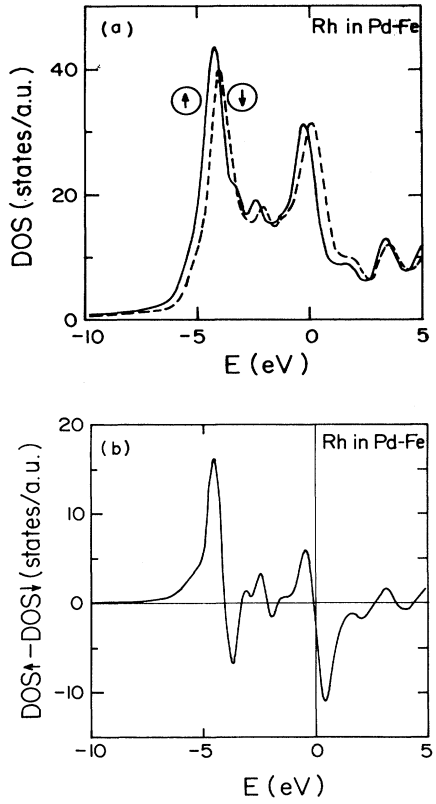

FIG. 5. (a) Local density of states (DOS) and (b) spin-difference density of states for a Rh atom in Pd matrix in the vicinity of a substitutional Fe atom at a distance $d = a$.

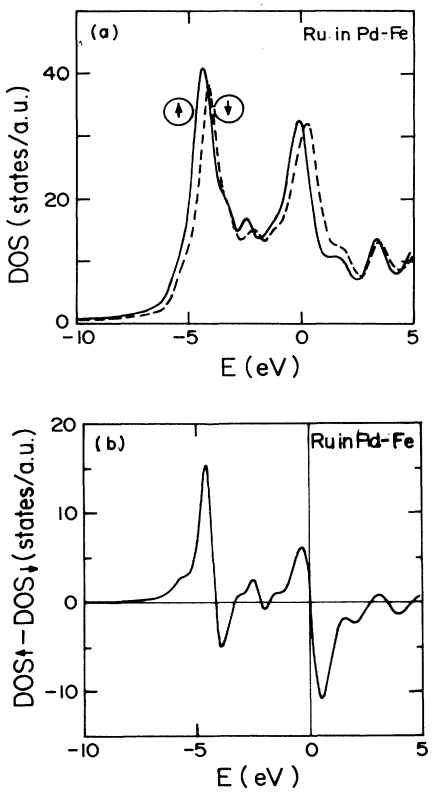

FIG. 6. (a) Local density of states (DOS) and (b) spin-difference density of states for a Ru atom in Pd matrix in the vicinity of a substitutional Fe atom at a distance $d = a$.

system. The Pd matrix atoms play a mediative role by providing a nearly filled d band; however, the strength and extent of the latter's polarization is the determining criterion for the stability of the local moment formed.

(3) A Rh or Ru probe atom decorated with two Fe atoms placed symmetrically opposite the probe at nn distance $d=a/\sqrt{2}=2.75$ Å. This situation, which also becomes prominent at even higher Fe concentrations, is different from and must not be mistaken for the case of single probe-single Fe atom interaction at nn distance in the Pd matrix, which we have not been able to study. The local d moments on both Rh and Ru are now reduced to 0.73 and $0.55\mu_B$ respectively, a consequence of the probe-Fe interaction now playing a greater role. The average d polarization $\langle\mu_{12}^d\rangle$ on the nn Pd atoms also decreases by $\sim 0.08\mu_B$ suggesting that it scales with the local impurity moment. Once again, the increase in μ_{tot} with decoration by $\gtrsim 2\mu_B$ over case (1) is due to the moment on the extra Fe atom, rather than a corresponding increase in the Pd polarizations.

In a recent TDPAC experiment, Khatua *et al.*[15] studied spin fluctuation and local magnetism of isolated ^{100}Rh ions in paramagnetic dilute Pd-Fe alloys having 0.2–2 % Fe in Pd. They obtained a Curie-Weiss-like local susceptibility response that reflected enhanced stability of the Rh moment in the presence of Fe, as indicated by the drastic reduction in spin-fluctuation (sf) rates and temperatures T_K down to 0 K. A net moment per probe atom, μ_{tot}, was also extracted from the data under reasonable assumptions. Further, the spin rotation spectra for alloys with $\gtrsim 1\%$ Fe could be fitted to a superposition of two frequencies: a primary component for which μ_{tot} was seen to grow gradually from $4.8\mu_B$ for Rh in pure Pd to $7\mu_B$ for Rh in $Pd_{0.99}Fe_{0.01}$, and a minority contribution, seen only at higher Fe concentrations, for which μ_{tot} is already large and jumps appreciably from ~ 8.2 to $\sim 13\mu_B$ in going from 1 to 2% Fe concentration. We can now identify the former as due to the probe Rh atom being in the polarization cloud of exactly one Fe atom, and the latter to decoration of the probe with successively more Fe atoms. A similar scenario has also been reported[25] for Ru in dilute Pd-Fe alloys.

IV. CONCLUSIONS

In summary, we have performed self-consistent electronic-structure calculations to investigate the possible existence and formation mechanism of local magnetism in isolated late-4d transition-metal impurities in Pd and dilute Pd-Fe alloys, using the local-spin-density approximation and the cluster model for simulating the bulk. Our calculations show that Ru in Pd exhibits a giant moment of $4\mu_B$, but reduced in magnitude compared to its 3d counterpart Fe in Pd. Tc and Rh in Pd turn out to be nonmagnetic, the latter in disagreement with TDPAC experiments which suggest a reduced giant moment per Rh atom. The prominent interaction, as in the magnetic 3d impurities in Pd, is ferromagnetic impurity-host d-d hybridization; additionally, the self-consistent small d-band splittings allow for an electronic exchange conversion growing in extent towards the center of the 4d series, i.e., some spin-up electrons are transferred to and accommodated in the minority-spin states near the Fermi energy. There is a consequent reduction in the impurity-site local moment and in the host-d spin polarization, as for Ru in Pd, and even a null moment result as for Tc in Pd. This compromised d-d interaction is less effective in suppressing the spin fluctuations from the impurity-host d-sp interaction and results in high spin-fluctuation temperatures T_K. This is the essential difference with 3d giant moment formation in Pd. Further, in very dilute Pd-Fe alloys, a local moment of $\sim 1\mu_B$ is seen to stabilize at a Rh or Ru probe site when in the polarization cloud surrounding an Fe atom. The enhancement in the exchange splitting and in the host-d polarization, resulting in an extensive polarization cloud with a giant moment, suggests a decrease in T_K. At higher Fe concentrations, decoration of the probe with Fe atoms results in polarization clouds with ultralarge stabilized local moments, also observed via TDPAC, which increase in jumps of at least the $\sim 3.4\mu_B$ d moment on each Fe atom.

[1]For data compilation, see *Landolt-Börnstein, New Series III/19a,* edited by K. H. Hellwege and O. Madelung (Springer-Verlag, Berlin, 1987). An earlier compilation is by K. H. Fisher, in *Landolt-Börnstein,* edited by K. H. Hellwege and J. L. Olson (Springer-Verlag, Berlin, 1982), Vol. 15, Group III, p. 289.

[2]H. E. Mahnke, Hyperfine Interactions **49**, 439 (1989); R. M. Steffen and H. Frauenfelder, in *Perturbed Angular Correlations,* edited by E. Karlsson, E. Matthias, and K. Siegbahn (North-Holland, Amsterdam, 1964), p. 15.

[3]See review articles by D. Riegel, Hyperfine Interactions **49**, 439 (1989); D. Riegel and K. D. Gross, Physica B **163**, 678 (1990).

[4]D. Riegel, K. D. Gross, and M. Luszik-Bhadra, Phys. Rev. Lett. **59**, 1244 (1987); D. Riegel, L. Büermann, K. D. Gross, M. Luszik-Bhadra, and S. N. Mishra, *ibid.* **61**, 2129 (1988); **62**, 316 (1989).

[5]J. Friedel, Can. J. Phys. **34**, 1190 (1956); P. W. Anderson, Phys. Rev. **124**, 41 (1961).

[6]J. Kondo, in *Solid State Physics,* edited by F. Seitz, D. Turnbull, and H. Ehrenreich (Academic, New York, 1969), Vol. 23, p. 183.

[7]G. Grüner, Adv. Phys. **23**, 941 (1974).

[8]D. Guenzburger and D. E. Ellis, Phys. Rev. Lett. **67**, 3832 (1991); Phys. Rev. B **45**, 285 (1992).

[9]For a recent review, see J. Callaway and N. H. March, in *Solid State Physics,* edited by H. Ehrenreich and D. Turnbull (Academic, New York, 1984), Vol. 38.

[10]R. Podloucky, R. Zeller, and P. H. Dederichs, Phys. Rev. B **22**, 5777 (1980); P. J. Braspenning, R. Zeller, A. Lodder, and P. H. Dederichs, *ibid.* **29**, 703 (1984); R. Zeller, J. Phys. F **17**, 2123 (1987).

[11]G. A. Benesh and D. E. Ellis, Phys. Rev. B **24**, 1602 (1981); D. E. Ellis, G. A. Benesh, and E. Byrom, *ibid.* **16**, 3308 (1977).

[12]V. L. Moruzzi, J. F. Janak, and A. R. Williams, *Calculated Electronic Properties of Metals* (Pergamon, New York, 1978), p. 144.

[13]A. Oswald, R. Zeller, and P. H. Dederichs, Phys. Rev. Lett. **56**, 1419 (1986).

[14]K. D. Gross, D. Riegel, and R. Zeller, Phys. Rev. Lett. **65**, 3044 (1990).
[15]S. Khatua, S. N. Mishra, S. H. Devare, and H. G. Devare, Phys. Rev. Lett. **68**, 1038 (1992).
[16]D. E. Ellis and G. S. Painter, Phys. Rev. B **2**, 2887 (1970); E. J. Baerends, D. E. Ellis, and P. Ros, Chem. Phys. **2**, 41 (1973).
[17]U. von Barth and L. Hedin, J. Phys. C **5**, 1629 (1972).
[18]J. A. Seitchik, A. C. Gossard, and V. Jaccarino, Phys. Rev. **136**, A1119 (1964).
[19]G. N. Rao, E. Matthias, and D. A. Shirley, Phys. Rev. **184**, 325 (1969).
[20]A. Narath and H. T. Weaver, Phys. Rev. B **3**, 616 (1971).
[21]B. Delley, D. E. Ellis, and A. J. Freeman, J. Magn. Magn. Mater. **30**, 71 (1982).
[22]A. P. Malozemoff, A. R. Williams, K.Terakura, V. L. Moruzzi, and K. Fukamachi, J. Magn. Magn. Mater. **35**, 192 (1983).
[23]G. Shirane, C. W. Chen, P. A. Flin, and R. Nathans, Phys. Rev. **131**, 183 (1963); G. Shirane, R. Nathans, and C. W. Chen, *ibid.* **134**, A1547 (1964).
[24]V. L. Moruzzi and P. M. Marcus, Phys. Rev. B **46**, 2864 (1992).
[25]D. Riegel, J. Kapoor, A. Metz, K. D. Gross, W. Brewer, and S. Hauf (private communication).